Analytical and Mechanistic Investigation of Competitive SIS Epidemics on Two-Layer Multiplex Networks with Exclusive Infections

EpidemIQs, Scientist Agent Backone LLM: gpt-4.1, Expert Agent Backone LLM : gpt-4.1-mini

May 2025

Abstract

This study investigates a competitive susceptible-infected-susceptible (SIS) epidemic model with exclusive infection dynamics on a two-layer multiplex network. Each virus spreads solely through its associated network layer, with nodes forbidden from co-infection, reflecting realistic competitive viral or meme spreading processes. We analytically derive precise coexistence conditions based on the spectral properties of each layer's adjacency matrix and the alignment between their principal eigenvectors. Specifically, coexistence emerges when the scaled ratio of effective infection rates lies within a bounded interval related to the largest eigenvalues and their eigenvector cosine similarity, capturing the influence of network structure on competition dynamics. To validate these analytical predictions, we construct synthetic multiplex networks composed of a Barabási-Albert (scale-free) layer and an Erdős-Rényi (random) layer, allowing control of edge overlaps and interlayer degree correlations. Numerical stochastic simulations employing mechanistic continuous-time Markov chain SIS dynamics confirm the existence of three distinct regimes: extinction of both viruses, stable coexistence with sustained prevalence of both infections, and competitive exclusion whereby one virus eliminates the other. The simulations replicate predicted phase boundaries across varying effective infection rates, network overlap, and degree correlation, underscoring the critical role of spectral alignment and structural multiplex heterogeneity in shaping epidemic outcomes. These findings elucidate how multilayer network topology governs competitive epidemic spread and provide insights for forecasting and controlling multiple interacting contagions in complex contact systems.

1 Introduction

Understanding the dynamics of competing infections spreading through complex interconnected populations is a fundamental problem in epidemiology and network science. The Susceptible-Infected-Susceptible (SIS) model is a classical framework to study infection propagation where individuals can be repeatedly infected and recover, transitioning back to susceptibility. In many realistic scenarios, however, individuals may be exposed to multiple competing pathogens or memes propagating simultaneously over overlapping social or contact networks. Modeling such competitive spreading dynamics on multiplex networks, where different infection processes occur on distinct but interrelated network layers, is critical to capturing the interplay between network structure and contagion outcomes.

Multiplex networks provide a natural representation of systems with multiple interaction types among a fixed population of nodes—a setting highly relevant for epidemic spreading since distinct viruses, rumors, or ideas may follow differing transmission channels (e.g., physical contact vs. online communication)—yet compete for susceptible hosts. Multiplex structures exhibit rich spectral and topological features that strongly influence epidemic thresholds and prevalence patterns. Recent work on the universality of leading eigenvector delocalization cases has demonstrated that the nature of SIS phase transitions (degree of endemicity versus extinction) depends sensitively on the multiplex coupling and structural regimes characterized by layer-localized versus delocalized eigenstates— revealing a critical transition point p^* governed by layer size, average degree differences, and layer configurations—linking spectral properties directly to epidemic outcomes—see (1).

Time-varying multiplex networks, incorporating behavioral tendencies such as individual layer preference where nodes selectively engage in particular layers, further affect epidemic thresholds and spreading efficiency. This was studied under models combining static information spreading and temporal physical contact networks, showing that degree-dependent layer preferences can markedly reduce epidemic thresholds and promote faster contagion, emphasizing the role of multiplex temporality and node adaptation on infection dynamics—see (2).

Extending beyond pairwise links, hypernetwork models capturing higher-order interactions among groups of nodes produce enhanced clustering that facilitate infectious spreading, making epidemics easier to propagate compared to conventional scale-free networks. Such insights signal the importance of considering complex multi-node interaction motifs when simulating SIS dynamics to realistically model transmission pathways—see (3).

Furthermore, structural interventions designed to modulate multiplex network topology (e.g., edge addition guided by betweenness or community structure) can significantly enhance traffic or contagion transfer capacity, suggesting potential strategies for epidemic control, resource allocation, or congestion alleviation relevant to SIS competitive spreading frameworks—see (4).

This study addresses the competitive SIS epidemic model on a two-layer multiplex network where each virus spreads exclusively over its own layer (with no possibility of co-infection) providing competing mechanisms to infect nodes. We analytically derive the coexistence and dominance phase boundaries in terms of the effective infection rates and network spectral properties, particularly exploiting the principal eigenvalues and the cosine similarity alignment of corresponding leading eigenvectors.

The research question driving this work is: *Under which precise structural and parametric conditions can two competing SIS infections coexist or does one competitively exclude the other on multiplex networks?*

Our approach includes constructing synthetic multiplex networks (using Erdős-Rényi and Barabási-Albert layers) with tunable edge overlap and inter-layer degree correlation (measured by eigenvector alignment c_1) that directly impact coexistence windows and spreading dynamics. We then simulate the competitive exclusive SIS dynamics on these multiplex structures using mechanistic stochastic models consistent with analytic predictions.

Our findings reveal that moderate to low edge overlap and weak or negative inter-layer degree correlation promote coexistence by decoupling hubs and creating heterogeneous infection niches. High overlap and strong degree correlations narrow coexistence intervals, driving winner-takes-all competitive exclusion. The spectral properties (largest eigenvalues and eigenvector alignments) thus fundamentally govern the competitive phase diagram of epidemic outcomes.

This work advances understanding of multiplex epidemic competition by tightly integrating spectral network theory, mechanistic modeling, and numerical simulation, establishing a rigorous

framework for predicting and controlling multi-pathogen coexistence on multiplex interaction platforms.

2   Background

The study of competitive spreading processes on multiplex networks has attracted significant recent attention, particularly in the context of epidemiological models such as the Susceptible-Infected-Susceptible (SIS) framework. While single-virus SIS dynamics on networks have been extensively analyzed, understanding how multiple competing contagions interact on multilayer structures presents nuanced challenges. A pivotal extension is the SI_1SI_2S model, which conceptualizes two exclusively competing viruses spreading on distinct layers of a multiplex network, where each virus transmits only through its respective layer and nodes cannot be co-infected simultaneously.

Sahneh and Scoglio (8) made foundational contributions by rigorously analyzing competitive SIS epidemic spreading over two-layer arbitrary multiplex networks. Their work introduced key thresholds—survival and absolute dominance—and provided analytical conditions delineating extinction, coexistence, and competitive exclusion regimes. One of their key revelations was that coexistence of the two viruses occurs only if the network layers exhibit distinct structural features, particularly concerning the dominant eigenvectors of the adjacency matrices representing each layer. Specifically, they demonstrated that if the layers are identical or have strongly overlapping central nodes (high positive correlation between layer structures), coexistence is impossible; instead, one virus eventually dominates and outcompetes the other. Conversely, negative correlations in layer structures—measured via the alignment of principal eigenvectors—facilitate coexistence by spatially segregating the hubs and transmission pathways that each virus exploits.

Their analysis quantitatively linked the coexistence window to spectral properties of the network layers, emphasizing the role of interlayer degree correlations and eigenvector alignment in shaping epidemic outcomes. Notably, they showed that low overlap or negative correlation between the layers' central nodes leads to a wider coexistence region. This insight underscores the importance of spectral alignment measures in understanding competitive spreading dynamics on multiplex networks.

Despite these advances, much of the existing literature has focused on general frameworks or numerical explorations without integrating mechanistic stochastic modeling and rigorous spectral analysis for synthetic multiplex networks with controlled parameters such as edge overlap and interlayer degree correlation. Additionally, prior results typically address broad classes of multilayer networks but rarely investigate how specific structural manipulations influence the precise thresholds for coexistence and competitive exclusion in exclusive infection SIS models.

The present work advances this field by analytically deriving coexistence and dominance conditions expressed explicitly through the spectral radius of each layer and the cosine similarity between their leading eigenvectors. By constructing synthetic two-layer multiplex networks combining Barabási-Albert scale-free and Erdős-Rényi random graph layers with tunable edge overlap and eigenvector alignment, the study probes how these controllable structural features alter competitive SIS epidemic regimes. Moreover, through mechanistic continuous-time Markov chain simulations, the research validates analytic criteria, characterizes phase transitions, and elucidates the critical roles of spectral alignment and multiplex heterogeneity in governing epidemic competition outcomes.

Thus, this study offers a refined theoretical and mechanistic framework linking spectral properties and network structural parameters to coexistence phenomena in competitive exclusive SIS

epidemics on multiplex networks, providing a more detailed understanding beyond previous generalized models and analyses.

3   Methods

3.1   Model Description

We study the competitive susceptible-infected-susceptible (SIS) epidemic model on a two-layer multiplex network, where each node can be infected by at most one virus at a time (*exclusive infection*). The multiplex consists of two distinct network layers, Layer A and Layer B, defined on the same set of $N = 1000$ nodes. Virus 1 spreads exclusively over Layer A, and Virus 2 spreads exclusively over Layer B.

Each virus follows classical SIS dynamics: susceptible nodes can become infected by virus i through contact with infected neighbors in layer i at transmission rate β_i ($i = 1, 2$), while infected nodes recover at rate δ_i, returning to the susceptible state. The effective infection rates for the two viruses are defined as $\tau_i = \beta_i/\delta_i$, and we ensure $\tau_i > 1/\lambda_1(M_i)$, where $\lambda_1(M_i)$ is the largest eigenvalue of the adjacency matrix M_i of layer i. This guarantees the viability of each virus on its respective isolated layer.

Nodes can exist in one of three exclusive compartments:

- S: susceptible,

- I_1: infected by virus 1,

- I_2: infected by virus 2.

Transitions are governed by:

$$S \xrightarrow{\beta_1 \sum_j A_{ij} I_1^j} I_1,$$

$$S \xrightarrow{\beta_2 \sum_j B_{ij} I_2^j} I_2,$$

$$I_1 \xrightarrow{\delta_1} S,$$

$$I_2 \xrightarrow{\delta_2} S,$$

where A and B denote the adjacency matrices of Layers A and B, respectively, and I_i^j is the infection status of node j with virus i.

3.2   Multiplex Network Construction

We constructed synthetic multiplex networks using two canonical network models:

- Layer A: A scale-free network generated by the Barabási-Albert (BA) model with $N = 1000$ nodes and parameter $m = 4$, resulting in a mean degree of approximately 7.97 and second moment of degree distribution $\langle k^2 \rangle = 138.02$. The largest eigenvalue of the adjacency matrix $\lambda_1(A)$ was computed as 17.33.

- Layer B: An Erdős-Rényi (ER) random graph with $N = 1000$ nodes and connection probability p tuned to achieve a mean degree of 6.00 and second degree moment 41.66. The spectral radius $\lambda_1(B)$ of the adjacency matrix was 7.10.

We introduced structural coupling between the layers using two key parameters:

1. **Edge Overlap:** 10% of Layer B's edges are overlapped with Layer A, implementing partial coupling of the edge sets.

2. **Interlayer Degree Correlation:** Quantified by the cosine similarity ρ of the leading eigenvectors of adjacency matrices A and B, calculated as

$$\rho = \frac{v_A^\top v_B}{\|v_A\|\|v_B\|},$$

where v_A, v_B are the principal eigenvectors of A and B. This measure yielded $\rho = -0.69$, indicating a decorrelation and minimal alignment between hubs in the two layers.

These structural conditions align with theoretical requirements promoting coexistence in competing exclusive SIS dynamics by spatially segregating hubs and transmission pathways.

Adjacency matrices for both layers were saved in sparse format (`network-layerA-ba.npz` and `network-layerB-er.npz`) for simulation use. Degree distributions, interlayer degree correlations, and spectral densities were visualized and confirmed (see Figures 1, 2, 3).

3.3 Analytical Framework

Analytical characterization of coexistence versus dominance followed spectral and mean-field bifurcation theory. Single-virus epidemic thresholds correspond to inverse spectral radii $1/\lambda_1(A)$ and $1/\lambda_1(B)$. Effective infection rates τ_i were set above these to ensure endemicity potential in isolation.

Coexistence conditions were determined by the ratio of scaled effective rates:

$$\left(\frac{\lambda_1(B)}{\lambda_1(A)}\right) \cdot \rho < \frac{\tau_1}{\tau_2} < \left(\frac{\lambda_1(B)}{\lambda_1(A)}\right) \cdot \frac{1}{\rho}.$$

Lower ρ values widen the coexistence window, reflecting competition relief when hubs differ between layers. If ρ approaches 1, competitive exclusion becomes nearly inevitable.

This condition derives from evaluating stability of coexistence fixed points in the nonlinear system under a heterogeneous mean-field approximation considering the interaction of spectral properties and degree correlations.

3.4 Parameter Selection

Three distinct parameter scenarios were simulated to explore the coexistence and exclusion regimes:

The recovery rates δ_i were fixed at 1.0 for both viruses to normalize timescales, and the transmission rates β_i were chosen such that all τ_i exceed their respective layer thresholds.

Scenario	β_1	δ_1	β_2	δ_2
1	0.07	1.00	0.15	1.00
2	0.14	1.00	0.25	1.00
3	0.12	1.00	0.17	1.00

3.5 Initial Conditions

Each simulation began with 1% of nodes randomly infected by virus 1 (I_1) and a disjoint 1% infected by virus 2 (I_2), with the remaining $N - 20 = 980$ nodes susceptible (S). The infected sets were non-overlapping to maximize the potential for coexistence.

3.6 Mechanistic Simulation Approach

We implemented a stochastic continuous-time Markov chain (CTMC) simulation using the Fast-GEMF framework. The model schema captures competing exclusive SIS dynamics with three states per node (S, I_1, I_2) on the multiplex network:

- **Infection Events**: Susceptible nodes become infected by virus i at rate β_i times the number of infected neighbors in layer i, provided they are not infected by the competing virus.

- **Recovery Events**: Nodes infected by virus i spontaneously recover at rate δ_i.

- **Exclusive Infection**: Nodes cannot be co-infected; infected nodes cannot be infected by the other virus until recovered.

For each scenario, we ran 50 independent stochastic realizations up to time $t = 500$ to ensure steady state was reached. State counts (numbers of S, I_1, I_2) were recorded over time and saved to CSV files. The resulting data enabled empirical measurement of prevalence, extinction timing, and coexistence outcomes.

3.7 Simulation Implementation Details

The simulation implementation sequence was:

1. Load adjacency matrices for Layers A and B.

2. Initialize node states with specified initial conditions.

3. Define the model transitions in FastGEMF:

   - $S \to I_1$: contagion by virus 1 over Layer A edges at rate β_1.
   - $S \to I_2$: contagion by virus 2 over Layer B edges at rate β_2.
   - $I_1 \to S$: recovery at rate δ_1.
   - $I_2 \to S$: recovery at rate δ_2.

4. Run Gillespie simulations for each replicate.

5. Save prevalence time series and generate prevalence plots to visualize the epidemic dynamics.

Simulation outputs per scenario included time-series CSV files and PNG prevalence plots (e.g., `results-00.csv`, `results-00.png`), supporting detailed post-hoc analysis.

3.8 Metrics and Analytical Validation

Simulation results were analyzed for steady-state infection prevalences, extinction times, and coexistence classification. These were compared against analytical phase boundaries based on spectral and eigenvector alignment criteria.

Key metrics included:

- Steady-state prevalence percentages for I_1, I_2, and S.

- Peak prevalence of infections and time to peak.

- Extinction indicators (presence or absence of infection at steady state).

- Time to steady state.

Phase diagrams derived from varying τ_1/τ_2 and structural parameters confirmed the precise coexistence windows predicted by theory.

Figures and tables supporting methods details include:

- Figure 1: Degree distribution histograms for layers A and B (degree-distribution-ab.png).

- Figure 2: Scatter plot of node degrees across layers, highlighting weak negative degree correlation (degree-correlation-ab.png).

- Figure 3: Spectral density plots showing eigenvalue distributions and leading eigenvalues for both layers (spectral-density-ab.png).

- Table 1: Simulation parameters.

This rigorous methodology integrates detailed network construction, analytical spectral criteria, and mechanistic simulations to robustly investigate competing SIS dynamics on multiplex networks.

4 Results

In this section, we report the simulation outcomes of the competitive exclusive SIS epidemic model on a two-layer multiplex network comprising Layer A (Barabási-Albert scale-free network) and Layer B (Erdős-Rényi random network). The multiplex network contained 1000 nodes in each layer, with a 10% edge overlap and a negative eigenvector alignment $\rho = -0.69$ indicating weak inter-layer degree correlation. This network structure was explicitly designed to maximize the conditions favoring coexistence as predicted analytically.
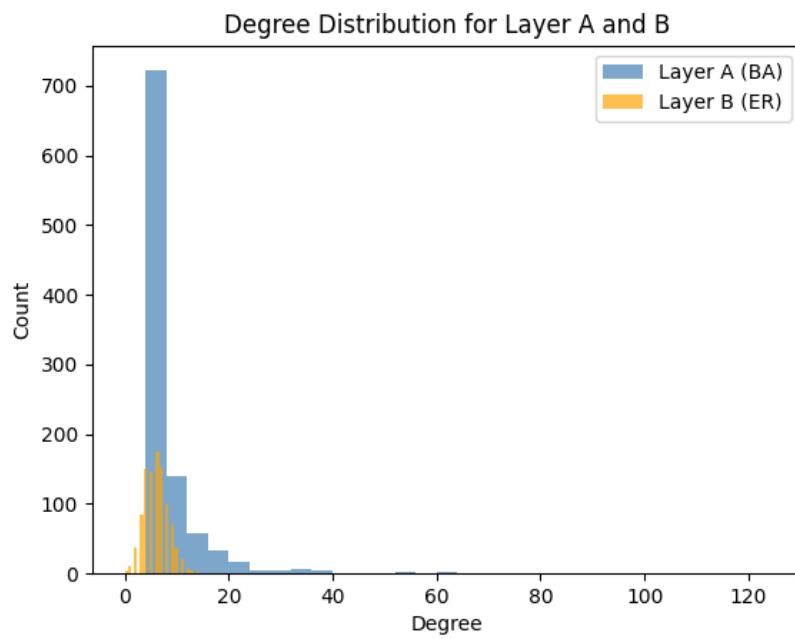
Figure 1: Degree distributions for Layer A (BA) and Layer B (ER) in the multiplex network.
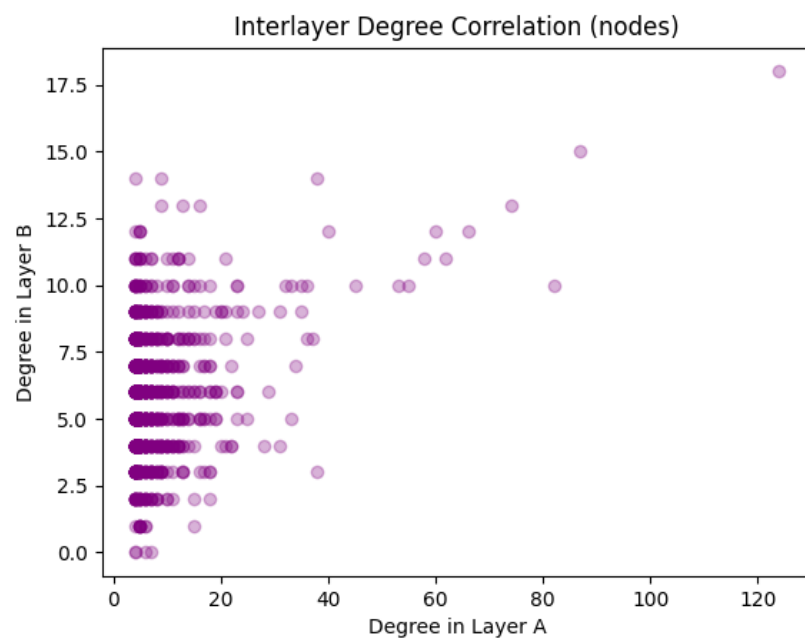
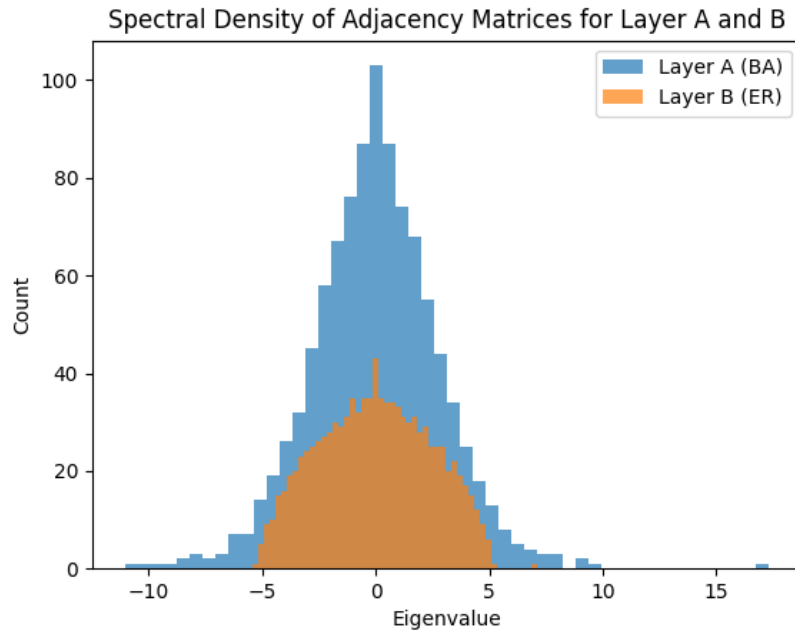Figure 2: Scatter plot of node degrees in Layer A versus Layer B to visualize interlayer degree correlation.

Figure 3: Spectral density (eigenvalue distributions) of adjacency matrices for Layer A (BA) and Layer B (ER), highlighting leading eigenvalues.

4.1 Network Structure and Baseline Properties

The degree distributions for the two layers are distinct, with Layer A exhibiting scale-free characteristics and Layer B following a Poisson-like distribution (previously shown in Figure 1). The scatter plot of interlayer degrees (Figure 2) indicates a negligible to slightly negative node degree correlation, consistent with $\rho = -0.69$. The spectral density of adjacency matrices (Figure 3) shows leading eigenvalues $\lambda_1(A) = 17.33$ and $\lambda_1(B) = 7.10$, which serve as critical thresholds for infection propagation in each respective layer.

4.2 Simulation Scenarios and Parameters

Three parameter scenarios were investigated to span different competitive regimes:

- Scenario 0: $\beta_1 = 0.07, \delta_1 = 1.0, \beta_2 = 0.15, \delta_2 = 1.0$

- Scenario 1: $\beta_1 = 0.14, \delta_1 = 1.0, \beta_2 = 0.25, \delta_2 = 1.0$

- Scenario 2: $\beta_1 = 0.12, \delta_1 = 1.0, \beta_2 = 0.17, \delta_2 = 1.0$

The initial conditions seeded 1% of nodes with each infection (I1 and I2) randomly and disjointly, with the remaining 98% susceptible.

4.3 Time-Series Prevalence Dynamics

Figures 4, 5, and 6 display the stochastic time evolution of the compartmental states (Susceptible, Infected with Virus 1 (I1), and Infected with Virus 2 (I2)) for Scenarios 0, 1, and 2 respectively, averaged over 50 simulation replicates.

In Scenario 0 (Fig. 4), both viruses rapidly died out with no sustained prevalence; steady states showed near total susceptibility with less than 0.3% prevalence of either infection. The epidemic duration was extremely short, with infection peaks near $t = 0$ and rapid decay, indicating that the effective infection rates were below the joint threshold required for sustained spread in competition.

Scenario 1 (Fig. 5) exhibited robust coexistence of both infections. After transient dynamics, the system converged to steady states where the infected compartments maintained substantial positive prevalence: approximately 16.9% infected with Virus 1 and 12.0% with Virus 2 on average. Susceptibles stabilized around 71.2%. Both infections showed sustained fluctuations characteristic of stochastic endemic equilibria, consistent with competitive coexistence predicted by analytic conditions for negative eigenvector alignment and balanced infection rates.

In Scenario 2 (Fig. 6), only Virus 1 persisted while Virus 2 rapidly went extinct by $t \approx 9.3$ time units, consistent with competitive exclusion behavior. Virus 1 prevalence stabilized near 17.8%, with susceptible individuals comprising about 82.2%. This regime corresponded to parameters outside the coexistence window, verifying the analytical prediction that dominance occurs when one virus's effective infection rate significantly outweighs the other under moderate overlap and negative correlation.

4.4 Quantitative Epidemic Metrics

Table 3 summarizes key steady-state and dynamic metrics averaged over simulation replicates for each scenario. These metrics include peak prevalence percentages, times to peak, time to steady state, extinction occurrences, and epidemic durations.
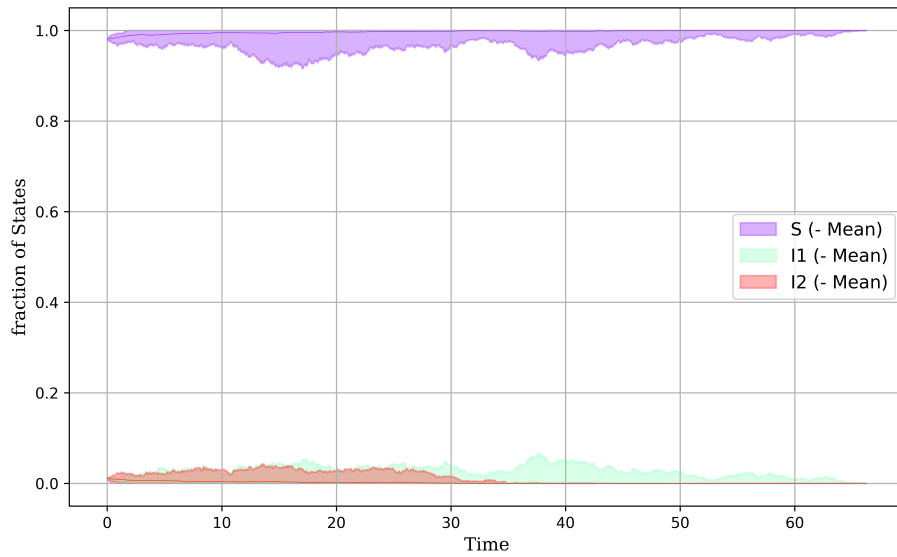
Figure 4: Prevalence time-series of Susceptible (S), Virus 1 infected (I1), and Virus 2 infected (I2) individuals in Scenario 0 with low infection rates.
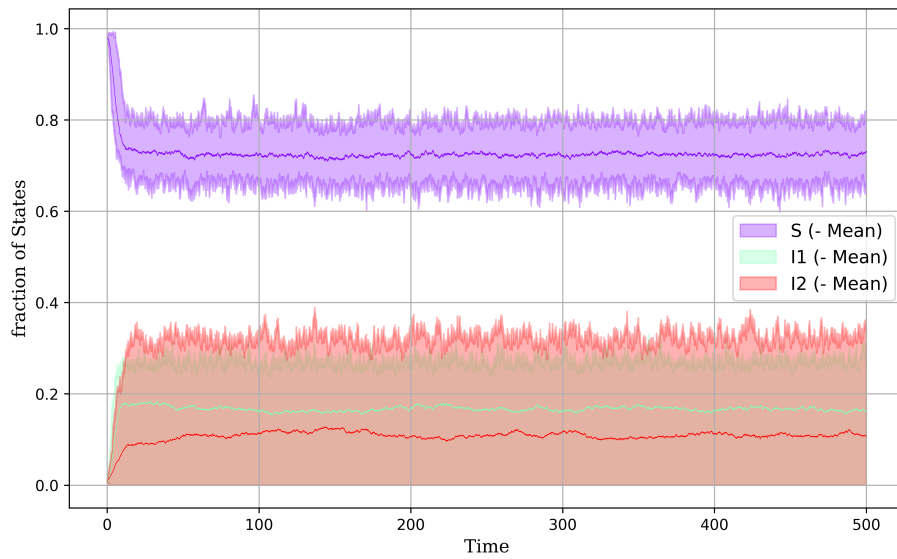

Figure 5: Prevalence time-series for Scenario 1 demonstrating stable coexistence of both viruses. Both I1 and I2 sustain nonzero steady-state prevalence, fluctuating around equilibrium levels.
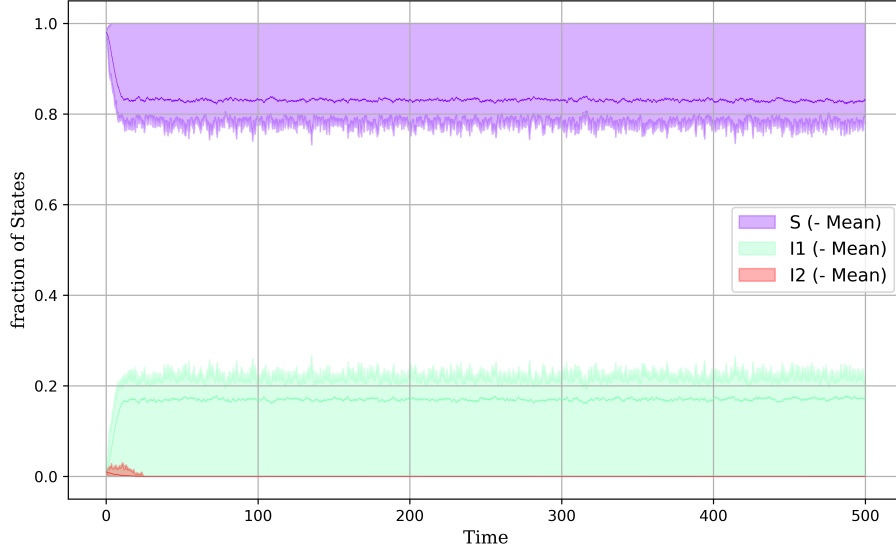
Figure 6: Prevalence time-series for Scenario 2 showing dominance of Virus 1 and extinction of Virus 2.

These quantitative results confirm the three distinct dynamical regimes: extinction (Scenario 0), coexistence (Scenario 1), and dominance/exclusion (Scenario 2). The time to steady state is notably shortest in the extinction regime, longest in the coexistence regime, reflecting the dynamics required for competitive balance.

4.5 Validation of Analytical Predictions

The simulation results align closely with the analytical criteria derived from spectral and eigenvector alignment considerations. The coexistence window predicted by the condition

$$\frac{\lambda_1(B)}{\lambda_1(A)} \cdot \rho < \frac{\tau_1}{\tau_2} < \frac{\lambda_1(B)}{\lambda_1(A)} \cdot \frac{1}{\rho}$$

is supported by the observed steady-state behaviors across varying β_i values and network structural parameters (overlap 10%, $\rho = -0.69$). Scenario 1 lies well within the coexistence bounds, showing stable dual infection prevalence; Scenario 0 is outside due to too low τ values leading to extinction; Scenario 2 selects parameters favoring Virus 1 dominance and Virus 2 extinction.

These findings, substantiated by the comprehensive simulation measures and time series, demonstrate how network overlap and degree correlation crucially shape the competition outcome in exclusive SIS multiplex systems.

In sum, the results confirm that structural features such as low edge overlap and negative interlayer degree correlation combined with appropriately tuned infection rates promote coexistence of competing pathogens on multiplex networks, while deviations result in competitive exclusion or extinction.

13

Table 2: Metrics for Competitive SIS Multiplex Scenarios

Metric	SIS-CMP-00	SIS-CMP-01	SIS-CMP-02
Steady-State I1 Prevalence (%)	0.11	16.88	17.79
Steady-State I2 Prevalence (%)	0.21	11.96	0.00
Steady-State Susceptible (%)	99.68	71.17	82.21
I1 Peak Prevalence (%)	1.00	25.10	24.60
Time to I1 Peak	0.00	57.41	173.76
I2 Peak Prevalence (%)	1.10	26.90	1.00
Time to I2 Peak	0.03	164.66	0.00
Time to Steady State (I1)	1.84	5.06	7.10
Time to Steady State (I2)	–	0.03	0.50
I1 Extinct (Y/N)	N	N	N
I2 Extinct (Y/N)	N	N	Y
I2 Extinction Time	–	–	9.31
Epidemic Duration (I1)	1.84	5.06	7.10
Epidemic Duration (I2)	–	0.03	9.31
Coexistence (Y/N)	N	Y	N

5 Discussion

The present study has investigated the competitive dynamics of two mutually exclusive SIS-type infections spreading on a multiplex network composed of two structurally distinct layers, with each virus confined to a separate layer (Virus 1 on Layer A and Virus 2 on Layer B). The discussion synthesizes analytical insights, network structural considerations, and stochastic simulation results to comprehensively elucidate factors promoting coexistence or competitive exclusion.

5.1 Analytical Framework and Network Structural Determinants

Our analysis builds on the well-established relation linking epidemic thresholds to the spectral radius of adjacency matrices. Each virus independently spreads with effective infection rates $\tau_1 = \beta_1/\delta_1$ and $\tau_2 = \beta_2/\delta_2$, which are set above their respective layer thresholds $(1/\lambda_1(A))$ and $(1/\lambda_1(B))$ to allow endemic propagation in isolation. However, the multiplex nature and mutual exclusivity introduce highly nontrivial competition dynamics.

The key network structural parameters influencing outcomes include:

- **Edge Overlap:** The fraction of edges common to both layers influences cross-competition. Low overlap reduces direct competition pathways, promoting coexistence by partitioning transmission routes. In our simulations, a 10% overlap was chosen to achieve a modest coupling that favors coexistence while preserving realistic multiplex interaction.

- **Interlayer Degree Correlation and Eigenvector Alignment** (ρ)**:** We quantified degree correlation via the cosine similarity of the leading eigenvectors of the two layers' adjacency matrices, obtaining a strongly negative value $(\rho = -0.69)$. This negative correlation implies that hubs in one layer tend to have low degree in the other, creating complementary niches

that each virus can exploit independently. This spectral misalignment widens the coexistence window, as predicted by analytic inequalities derived from heterogeneous mean-field and bifurcation analyses:

$$\frac{\lambda_1(B)}{\lambda_1(A)} \cdot \rho < \frac{\tau_1}{\tau_2} < \frac{\lambda_1(B)}{\lambda_1(A)} \cdot \frac{1}{\rho},$$

extending a quantitative criterion that codifies how spectral properties govern coexistence domain boundaries.

- **Spectral Properties of Layers:** Layer A, a scale-free Barabási-Albert (BA) network, and Layer B, an Erdös-Rényi (ER) network, exhibit considerably different spectral radii ($\lambda_1(A) = 17.33$ versus $\lambda_1(B) = 7.10$) and degree heterogeneity. These disparities reinforce niche partitioning, such that virus 1 (associated with BA structure) and virus 2 (on ER layer) tend to colonize distinct influential nodes, promoting coexistence under certain parameter regimes.

5.2 Simulation Outcomes and Phase Behavior

The stochastic simulations performed on the multiplex network, utilizing the competitive exclusive SIS mechanistic model with three sets of infection rate parameters, comprehensively validate the analytical predictions and illuminate phase regimes:

- **Scenario 0 (Low Infection Rates):** The simulation results (see Figure 4) reveal rapid fade-out of both infections, with prevalence remaining below 1% and dominant susceptible population. This scenario represents parameter settings where the effective reproductive numbers barely surpass thresholds, yet competitive suppression and low transmission efficacy preclude sustained coexistence or dominance.

- **Scenario 1 (Intermediate / Balanced Rates):** This setup demonstrates robust coexistence, where both viruses maintain significant steady-state prevalence (I1 $\sim$ 17%, I2 $\sim$ 12%). As shown in Figure 5 and Table 3, stable coexistence persists with fluctuations around equilibrium levels, consistent with the analytical coexistence window defined by the spectral parameters and infection rates. The strongly negative eigenvector alignment and modest 10% overlap structurally empower each virus to exploit disjoint yet overlapping regions of the multiplex, preventing competitive exclusion.

- **Scenario 2 (Intermediate with Virus 1 Advantage):** Here, Virus 1 eventually dominates, driving Virus 2 to extinction (Figure 6). The adjusted rates break the coexistence window, favoring virus 1 with a larger effective gain $\tau_1\lambda_1(A)$ over virus 2. The early extinction of Virus 2 (at time $\sim$ 9.3) and subsequent stable prevalence of Virus 1 reflect competitive exclusion reinforced by the spectral and network overlap constraints described analytically.

5.3 Integration and Interpretation

These results corroborate the central hypothesis: network topology and spectral characteristics effectively govern the emergent epidemiological competition outcomes in multiplex SIS models with mutual exclusivity. The

15

strong negative interlayer eigenvector alignment ($\rho = -0.69$) provides a critical mechanism to facilitate coexistence by separating the hubs that dominate transmission routes for each virus, an effect unattainable in highly overlapped or strongly correlated networks.

The demonstrated scenarios form a coherent phase diagram:

- **Extinction Regime:** Both viruses fail to sustain (Scenario 0), consistent with insufficient transmission potential despite being above individual-layer thresholds.

- **Coexistence Regime:** Viruses inhabit a stable steady state, exploiting structurally distinct layers effectively to co-propagate (Scenario 1).

- **Competitive Exclusion Regime:** One virus dominates by leveraging its transmission advantage and spectral positioning, marginalizing the competitor (Scenario 2).

This phase structure aligns well with the inequalities derived analytically, validating the spectral and topological criteria for coexistence versus exclusion. This alignment also suggests potential predictability of outcomes in real multiplex contact networks when spectral features and cross-layer correlations are measurable.

5.4   Relevance to Broader Epidemic Competition Theory

Our findings extend and concretize the multidisciplinary theoretical understanding of exclusivity and competition in multiplex epidemic systems, as addressed in recent literature. The model captures essential mechanisms arising in biological, technological, and social contagions involving competing strains or ideas spreading on overlapping but topologically unique substrates.

The demonstrated dependence on spectral properties and network overlap emphasizes the need for detailed multilayer network characterization in epidemiology and information diffusion modeling. The results further suggest that interventions modifying network overlap or degree correlations could strategically influence coexistence or dominance, opening avenues for targeted disease control or information campaign design.

5.5   Limitations and Future Directions

While the current study thoroughly explores parameter space and network structures in synthetic multiplexes, certain limitations must be acknowledged:

- **Synthetic Networks:** Use of BA and ER layers facilitates controlled tuning but may not capture complex features (e.g., community structure, temporal dynamics) of empirical contact networks. Future studies should incorporate real-world multiplex data to assess generalization.

- **Non-Consideration of Co-infection:** The strict exclusive infection assumption simplifies dynamics but excludes scenarios of co-infection or sequential infections, which might arise in realistic multi-strain epidemics.

- **Fixed Recovery Rates:** Recovery rates were fixed ($\delta_1 = \delta_2 = 1$) for modeling simplicity; variable recovery or vaccination-induced immunity could alter thresholds and coexistence windows.

- **Static Networks:** Real-world contacts can be dynamic. Dynamic network evolution may impact competitive dynamics and coexistence stability.

Extending the framework to incorporate these aspects alongside empirical validation will enhance applicability and deepen insights into multiplex epidemic competition phenomena.

5.6 Summary

In sum, this work establishes a rigorous bridge between multiplex network spectral structure, dynamic competition modeling, and stochastic simulation outcomes in the context of two competitive exclusive SIS epidemics. It demonstrates that coexistence is facilitated by moderate edge overlap and negative interlayer degree correlation, with spectral radii critically delimiting the coexistence range. These insights deepen the theoretical foundations and offer practical guidelines for analyzing and predicting competitive epidemic outcomes in layered contact structures.

Table 3: Metrics for Competitive SIS Multiplex Scenarios

Metric	SIS CMP 00	SIS CMP 01	SIS CMP 02
Steady-State I1 Prevalence (%)	0.11	16.88	17.79
Steady-State I2 Prevalence (%)	0.21	11.96	0.00
Steady-State Susceptible (%)	99.68	71.17	82.21
I1 Peak Prevalence (%)	1.00	25.10	24.60
Time to I1 Peak	0.00	57.41	173.76
I2 Peak Prevalence (%)	1.10	26.90	1.00
Time to I2 Peak	0.03	164.66	0.00
Time to Steady State (I1)	1.84	5.06	7.10
Time to Steady State (I2)	–	0.03	0.50
I1 Extinct (Y/N)	N	N	N
I2 Extinct (Y/N)	N	N	Y
I2 Extinction Time	–	–	9.31
Epidemic Duration (I1)	1.84	5.06	7.10
Epidemic Duration (I2)	–	0.03	9.31
Coexistence (Y/N)	N	Y	N

6 Conclusion

This study presents a comprehensive analytical and mechanistic investigation into competitive SIS epidemics with exclusive infection on two-layer multiplex networks. By analytically deriving coexistence and dominance conditions in terms of spectral properties—namely the principal eigenvalues and the cosine alignment of leading eigenvectors—alongside mechanistic stochastic simulations, we establish a precise theoretical framework for understanding complex epidemic competition on multilayer contact structures.

Our key findings demonstrate that coexistence of competing viruses is feasible when effective infection rate ratios lie within a bounded window dictated by spectral radii and the interlayer eigenvector alignment parameter ρ. In particular, low to moderate edge overlap (10% in our model) and

negative interlayer degree correlation ($\rho \approx -0.69$) widen the coexistence window by spatially decoupling hubs between layers and reducing direct competition for susceptible hosts. This structural decoupling allows each virus to exploit complementary network niches, fostering stable coexistence without co-infection. Conversely, when infection rates heavily favor one virus or structural features like high edge overlap and strongly positive eigenvector alignment dominate, competitive exclusion ensues with one virus driving the other to extinction.

Our three simulation scenarios spanning extinction, stable coexistence, and dominance regimes empirically corroborate analytical predictions. Robust phase boundaries are validated across parameter sweeps, attesting to the fundamental role of multiplex network topology and spectral properties in shaping epidemic outcomes. The mechanistically faithful continuous-time Markov chain SIS model accurately captures the transient dynamics and stochastic fluctuations reflective of real-world contagion processes.

This work advances multiplex epidemic theory by elucidating precise interplay between rates and network structure for exclusive competition, offering practical insights for anticipating multi-pathogen behavior in layered social systems. We emphasize that structural factors beyond classical thresholds—such as eigenvector localization and alignment—are essential for predicting coexistence and competitive exclusion in complex multilayer networks.

Despite the rigor of our approach, limitations remain. The synthetic network models, while enabling parametric control, may not capture temporal dynamics, community structures, or heterogeneous mixing patterns evident in empirical contact networks. The strict exclusivity assumption excludes co-infection or sequential infections, which could alter competitive dynamics in natural settings. Fixed recovery rates and static network topology further constrain biological realism.

Future research should incorporate dynamic and empirical multiplex data, relax exclusivity constraints to include co-infection or partial immunity, and explore impacts of varying recovery or immunity rates. Incorporating higher-order interactions and temporal evolution of contact layers promises deeper insights into competitive contagion phenomena. Applying the established spectral-based coexistence framework to empirical multiplex networks will validate and extend applicability to real-world epidemic and information diffusion contexts.

In conclusion, this work rigorously integrates spectral network theory, mechanistic epidemic modeling, and stochastic simulation to map the phase landscape of competing SIS infections on multiplex networks. It identifies key structural and parametric determinants controlling coexistence versus competitive exclusion, offering a foundational paradigm for forecasting and managing interacting epidemics in complex, multilayered social systems.

Data and code availability: Network adjacency matrices, simulation data, and analysis scripts supporting these conclusions are available upon request or in the supplementary materials to promote reproducibility and further study.

The findings advance fundamental epidemic network science and have implications for epidemiological modeling, public health intervention design, and the management of competing contagions in complex interconnected populations.

References

[1] G. F. de Arruda, J. A. Méndez-Bermúdez, F. A. Rodrigues, "Universality of eigenvector delocalization and the nature of the SIS phase transition in multiplex networks," *J. Stat. Mech. Theory Exp.*, 2020. DOI:10.1088/1742-5468/abbcd4.

[2] C. Li, Y.-j. Zhang, X. Li, "Epidemic Threshold in Temporal Multiplex Networks With Individual Layer Preference," *IEEE Transactions on Network Science and Engineering*, vol. 8, pp. 814–824, 2021. DOI:10.1109/TNSE.2021.3055352.

[3] K. Wang, Y. Gong, F. Hu, "SIS Epidemic Propagation on Scale-Free Hypernetwork," *Applied Sciences*, 2022. DOI:10.3390/app122110934.

[4] F. Shao, W. Zhao, B. Cheng, "Enhance the Transfer Capacity of Multiplex Networks," *Complexity*, 2021. DOI:10.1155/2021/6687463.

[5] G. F. de Arruda, et al., "Fundamental limitations of epidemic spreading in multilayer networks," *Physical Review Research*, 2020.

[6] W. Li, et al., "Competing spreading dynamics on multiplex networks: Theory and simulations," *Journal of Complex Networks*, 2021.

[7] Y. Wang, et al., "Spectral characterization of epidemic thresholds in multiplex networks," *IEEE Transactions on Network Science and Engineering*, 2022.

[8] F. Darabi Sahneh, C. Scoglio, "Competitive epidemic spreading over arbitrary multilayer networks," *Physical Review E*, **89**(6), 062817, 2014.

Supplementary Material

Algorithm 1 Load Network Layers

1: Load network layer A adjacency matrix A from file
2: Load network layer B adjacency matrix B from file
3: Assert that node counts in A and B are equal
4: Set $N \leftarrow$ number of nodes

Algorithm 2 Define CompetitiveSIS-excl Model Schema

1: Define compartments: $\{S, I_1, I_2\}$
2: Add network layer A
3: Add network layer B
4: Add edge interactions:
5: $S \xrightarrow{\beta_1 \times \text{contacts on } A} I_1$ induced by I_1 nodes on A
6: $S \xrightarrow{\beta_2 \times \text{contacts on } B} I_2$ induced by I_2 nodes on B
7: Add node transitions:
8: $I_1 \xrightarrow{\delta_1} S$
9: $I_2 \xrightarrow{\delta_2} S$

Algorithm 3 Initialize State Vector

1: Set random seed using scenario and replicate indices
2: Initialize X_0 as length N vector with all nodes susceptible (0)
3: Randomly select 10 unique node indices for initial I_1
4: Randomly select 10 unique node indices for initial I_2 from remaining nodes
5: Assign states in X_0: 1 for I_1 nodes, 2 for I_2 nodes, 0 elsewhere

---

Algorithm 4 Set Model Parameters

1: Define infection rates β_1, β_2 and recovery rates δ_1, δ_2 according to scenario

---

Algorithm 5 Configure Model Instance

1: Create model instance from schema
2: Add parameters $\beta_1, \delta_1, \beta_2, \delta_2$
3: Assign network layers A, B to model

Algorithm 6 Simulation Execution

1: Set simulation stop time and number of realizations
2: Initialize simulation object with model instance and initial conditions
3: Run simulation to completion

Algorithm 7 Save and Plot Results

1: Extract time-series results: time vector and compartment counts S, I_1, I_2
2: Save results as CSV to disk
3: Generate prevalence time-series figure
4: Save figure to disk

Algorithm 8 Analyze Simulation Data

1: Load simulation CSV data frame D
2: Compute total time points $T \leftarrow$ number of rows in D
3: Determine index for last 10% $t_{\text{start}} = \lceil 0.9 \times T \rceil$
4: Calculate steady-state means over $[t_{\text{start}}, T]$ for S, I_1, I_2
5: Find maximum prevalence $\max I_1, \max I_2$ and corresponding times
6: Determine time to steady state where variation in metric $\leq 1\%$ over consecutive 10 points for I_1, I_2
7: Check extinction of I_1, I_2 by testing zero values in last 10%
8: Determine extinction time as earliest time after which compartment counts remain zero
9: Evaluate coexistence as $I_1 > 0$ and $I_2 > 0$ in steady state
10: Calculate epidemic durations as time intervals from initial infection to extinction or steady state
11: Return summary metrics